P8.6 A MULTIPLE-WAVELENGTH POLARIMETRIC ANALYSIS OF THE 16 MAY 2010 OKLAHOMA CITY EXTREME HAILSTORM

JOSEPH C. PICCA* AND ALEXANDER V. RYZHKOV
Cooperative Institute for Mesoscale Meteorological Studies, University of Oklahoma, and NOAA/OAR National Severe Storms Laboratory, Norman, OK

1. INTRODUCTION

On the afternoon of 16 May 2010, an extremely damaging supercell thunderstorm produced hail across a large swath of central Oklahoma, including significant portions of the Oklahoma City metro area. Hail diameters up to softball-size (~10.8 cm) were reported, along with hail drifts reaching nearly 1.5 m in height. Total damage costs from the storm were estimated to be in the hundreds of millions of dollars. Additionally, several people caught outside were injured by falling hailstones

The extreme nature of this storm, as well as its location, presents a very unique case for analysis. Both S-band (KOUN) and C-band (OU-PRIME) polarimetric radars in Norman, Oklahoma sampled the storm at relatively close ranges (less than 60 km). Furthermore, the location of the supercell to the northwest of the radar sites ensures that fairly accurate radial comparisons of the data are possible, considering that KOUN and OU-PRIME lie only 6.9 km apart on a 157.3˚ / 337.3˚ axis. Subsequently, differences in the polarimetric variables between the two radars reveal quite significant information in terms of the bulk microphysical properties of the observed hydrometeors.

Perhaps of greatest importance for this particular case is the storm's track over such a highly populated area. This study takes advantage of an increased number of ground-truth hail reports, which is much higher than typically available with any one hailstorm (Fig. 1).

1.1 Synoptic Overview

During the daytime hours of 16 May 2010, a poorly-defined warm front slowly progressed northward through Oklahoma. Afternoon surface conditions south of the front were characterized by temperatures above 21˚C with dew points around 17-19˚C. In combination with an approaching upper-level disturbance, CAPE values around 2500 J kg^{-1} created quite favorable conditions for the development of severe thunderstorms with the potential to produce large hail.

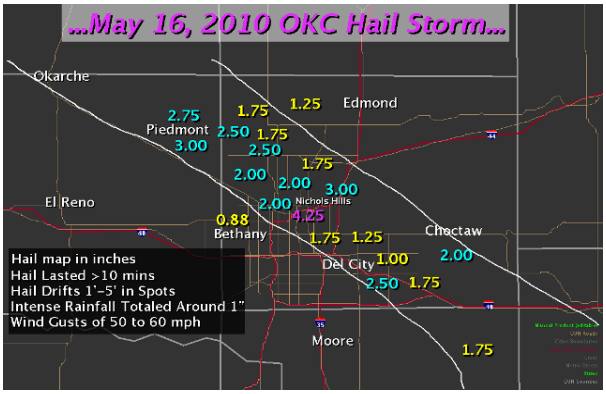

Fig. 1: Local storm reports of hail sizes across central Oklahoma during the afternoon of 16 May 2010 (NWS Norman).

Radar	KOUN	OU-PRIME
Wavelength	10.9 cm	5.44 cm
Azimuthal Resolution	1.0˚	0.5˚
Range Resolution	250 m	125 m
Elevation Angles	0.5˚, 0.9˚, 1.4˚, 1.8˚, 2.4˚, 3.2˚, 4.0˚, 5.1˚, 6.4˚, 8.0˚, 10.0˚, 12.5˚, 15.6˚, 19.5˚ (14 total)	0.25˚, 1.0˚, 2.0˚, 3.0˚, 4.0˚, 5.0˚, 6.5˚, 9.0˚ (8 total)
Update Time	261 s	145 s

Table 1: Scanning details for the two radars utilized in this study.

Around 1800 UTC, a supercell thunderstorm rapidly developed over Major County and "giant" hail reports (> 5 cm in diameter) quickly followed, with sizes of 7 cm and 10.8 cm in Major and Blaine counties, respectively, between 1800 and 1900 UTC. The supercell progressed southeast through central Oklahoma, where hail reports of at least golfball-size (> 4.4 cm) were frequent, with several reports over 5 cm.

Severe damage to automobiles, buildings, and vegetation was common along the storm's path through the metropolitan area, especially in Oklahoma County. Eventually, as the storm progressed farther southeast, hail sizes began to

* *Corresponding author address*: Joseph C. Picca, 120 David L. Boren Blvd., National Weather Center Suite 4900, Norman, OK 73072. Email: jpicca@ou.edu

decrease in Seminole, Hughes, Coal, and Atoka counties. Nonetheless, the storm left in its wake a very wide hail swath that stretched across Oklahoma from the second northernmost tier of counties to the second southernmost tier.

1.2 Data Collection

The data for this study were collected by the research polarimetric prototype WSR-88D (KOUN) and OU-PRIME, a 5-cm wavelength (C band) research polarimetric radar.

Data from OU-PRIME were acquired across a 93˚ sector with 8 elevation angles and an azimuthal resolution of 0.5˚. KOUN data were collected in a more standard volume coverage pattern (VCP) with 14 elevation angles and did not employ sector scanning. Due to the differences in scanning strategies, the data between the two radars are not synchronized. Nonetheless, the relative temporal proximity of the scans (generally less than 2 minutes) is sufficient for a comparative analysis. Further details of the two radars are provided in Table 1.

2. RADAR OBSERVATIONS OF HAIL REGIONS

At approximately 2100 UTC, the hailstorm reached a peak in intensity, and hailstones of baseball size and greater (> 7 cm) fell across portions of northwest Oklahoma City, including Penn Square Mall, where numerous automobiles in the mall parking lots were greatly damaged. Polarimetric data for this time display many particular features that are a result of the intense size and number of falling hailstones (Fig. 2). This study utilizes KOUN data as a first reference, as S band radiation is less affected by attenuation and resonance scattering. Observations from KOUN are then compared to the OU-PRIME data.

2.1 Low-level Hail Signature

2.1.1 S Band

At S band, the intense nature of the hail core is quite apparent, as 0.5˚ PPI reflectivity Z_H values exceed 65 dBZ over a sizeable area (Fig. 2). Within the core, Z_H values reach a maximum at 72.5 dBZ, which certainly indicates the presence of very large hail. Furthermore, this maximum is displaced well into the forward flank of the supercell. The location of these >70 dBZ values speaks to the extreme strength and organization of the cell updraft, which allowed very large hail to fall relatively far away from the inflow region.

Within the 60 dBZ contour an extensive region of depressed differential reflectivity Z_{DR} (≤ 0.5 dB) and low cross-correlation coefficient ρ_{hv} (generally ≤ 0.95) is observed. These values are a clear signature of severe hailstones (> 2.5 cm diameter) (e.g., Aydin et al. 1986; Balakrishnan and Zrnić 1990**)** falling across an extremely wide swath within the supercell.

Two regions of negative Z_{DR} are also apparent (-1 dB < Z_{DR} < 0 dB). The first exists to the west and southwest of the inflow notch, while the second exists to the northeast well within the forward flank. In the first region, Z_{DR} drops as low as -0.6 dB, while corresponding Z_H ranges between 62 dBZ and 66 dBZ. A quick glance at Fig. 2 subsequently indicates that the most negative Z_{DR} is not associated with the highest Z_H in the rear flank of the cell, as a zone of Z_H > 68 dBZ is present.

In the second region, Z_{DR} reaches a minimum of -0.75 dB, with corresponding Z_H ranging between 65 dBZ and 68 dBZ. Yet again, while near the zone of maximum Z_H > 72 dBZ (within 1.5-2 km range), the lowest Z_{DR} corresponds with Z_H approximately 4-6 dBZ less than the maximum.

In their calculation of Z_{DR} dependencies on hail size, Kumjian et al. (2010) show that negative Z_{DR} is associated with hail of D > 4-5 cm. Although not associated with the highest Z_H with this cell, the presence of Z_{DR} values near -0.6 dB to -0.7 dB within a region of high Z_H is indicative of hailstones around 5-6 cm. Our C band analysis to follow in section 2.1.2 serves to support this conclusion. It should be cautioned, however, that positive Z_{DR} does not preclude the presence of very large hailstones, as with both dry and wet hail, resonance first occurs at horizontal polarization, causing a peak in Z_{DR} around 3-4 cm and 5 cm for wet and dry hailstones, respectively.

Fig. 3 is a scatterplot representing the intense precipitation core at 2059 UTC. Overall, near-surface data within the core show a majority of points with positive Z_{DR}. As Z_H increases, Z_{DR} tends to become less positive, which is expected with the presence of hailstones. At higher values of Z_H (generally > 63 dBZ), there is a protrusion to negative Z_{DR} values, which again are likely associated with very large hailstones. Finally, we also observe a few points indicating negative Z_{DR} with Z_H < 60 dBZ. Kumjian et al. (2010) discuss how the largest hailstones within a cell tend to fall in regions of relatively low Z_H due to their small number concentration. Therefore, the presence of very large hailstones should not be discounted even if Z_H values are not exceptionally high.

Before switching focus to C band observations, we will briefly note the apparent Z_{DR} arc (zone of Z_{DR} > 3 dB along forward flank Z_H gradient) along and slightly north of y = 35 km. Z_{DR} arcs have been documented in the literature (e.g., Kumjian and Ryzhkov 2008) and are a result of an accumulation of large raindrops due to size sorting, which can reveal important environmental conditions such as storm-relative helicity (Kumjian and Ryzhkov 2008b).

For the purposes of the current analysis, however, the presence of numerous large drops, which is signaled by Z_{DR} upwards of 6 dB, is quite significant as C band observations of the forward flank hail core exhibit anomalously high attenuation, which will be detailed in the next section.

2.1.2 C Band

At C band, Z_H is noticeably lower than at S band by as much as 10 dBZ throughout the hail core, which is evidence that numerous hailstones of at least marginally severe sizes (> 2.5 cm) are present. This discrepancy in Z_H is similar to the "hail signal" from past studies that utilized the ratio of S- and X-band reflectivities to identify regions of hail (Atlas and Ludlam 1961; Eccles and Atlas 1973).

In areas of rain (outside the hail core), more expansive regions of > 5 dB Z_{DR} exist at C band than at S band. This difference results from the presence of large drops which causes resonance at the horizontal polarization for C band and greatly increases values. The effect is most evident in the Z_{DR} arc, where a large region of > 6 dB values exists, with a maximum as high as 7.5 dB.

Also at C band, pockets of higher Z_{DR} (> 2 dB) are noted within the hail core, which has been observed in many cases at 5-cm wavelength (Ryzhkov et al. 2007). Due to the shorter wavelength relative to S band, resonance scattering caused by large raindrops, many of them originating from smaller melting hailstones (< 3-4 cm), contributes to increased Z_{DR} values. As these hydrometeors are the dominant scatterers within a sampling volume, the lower intrinsic Z_{DR} of the hailstones themselves is masked (e.g. Borowska et al. 2010).

Also at C band, very low ρ_{hv} (much lower than at S band) exists throughout the hail core, which once again is a result of resonance scattering from both liquid drops and hailstones.

When investigating the data from the two radars, we can observe the great benefits possible from directly comparing two wavelengths and applying the results to each individual wavelength. Z_{DR} and ρ_{hv} at C band indicate two regions where giant hail is very likely falling (Fig. 2). As has already been mentioned, Z_{DR} typically remains higher (> 2 dB) within hail cores at C band as a result of the dominance of resonance scattering from liquid drops. However, in these regions values drop below 0 dB, indicating a high enough concentration of sufficiently large hailstones such that their backscatter contribution dominates and reduces overall Z_{DR}. Furthermore, we observe minima in ρ_{hv} within these regions as well (< 0.7), further supporting the likelihood of hail larger than 5 cm in diameter. Lastly, the regions of low Z_{DR} and ρ_{hv} to the northwest of region 1 and northeast of region 2 are not indicating giant hail, but rather are a result of overwhelming differential attenuation, which is apparent from their radial nature and location on the backside of the Z_H core. Additionally, nonuniform beam filling (NBF) caused by strong gradients of differential phase Φ_{DP} contributes to the radial "valleys" of reduced ρ_{hv}.

Interestingly, neither of these two regions appears to be associated with the highest Z_H within the core at C band. Therefore, it seems probable that the largest hailstones do not have to be associated with the highest Z_H values, further proving the utility of polarimetric radar versus conventional single-polarized radar.

By comparing these highlighted areas with KOUN data, we observe that the same regions at S band are characterized by either quite low Z_{DR} (< 0 dB) or ρ_{hv} (< 0.9). Therefore, it certainly appears that negative Z_{DR} and ρ_{hv} less than 0.9 at S band are associated with giant hailstones (> 5 cm). Once again, these regions are not associated with the highest Z_H observed at S band, proving that Z_{DR} and ρ_{hv} offer significant benefits in hail detection and sizing when used in conjunction with Z_H.

One can certainly see from these conclusions how this case displays the importance of research utilizing observations at multiple wavelengths and then applying the findings to the individual wavelengths for future operational purposes.

2.2 Attenuation / Differenial Attenuation at C Band

To compare data for each wavelength in more detail, we match two sets of azimuths (shown in Fig. 2) for each radar and plot the radial profiles of Z_H, Z_{DR}, and ρ_{hv}. These specific azimuths were selected because they provide the most direct radial comparisons. Although none of these

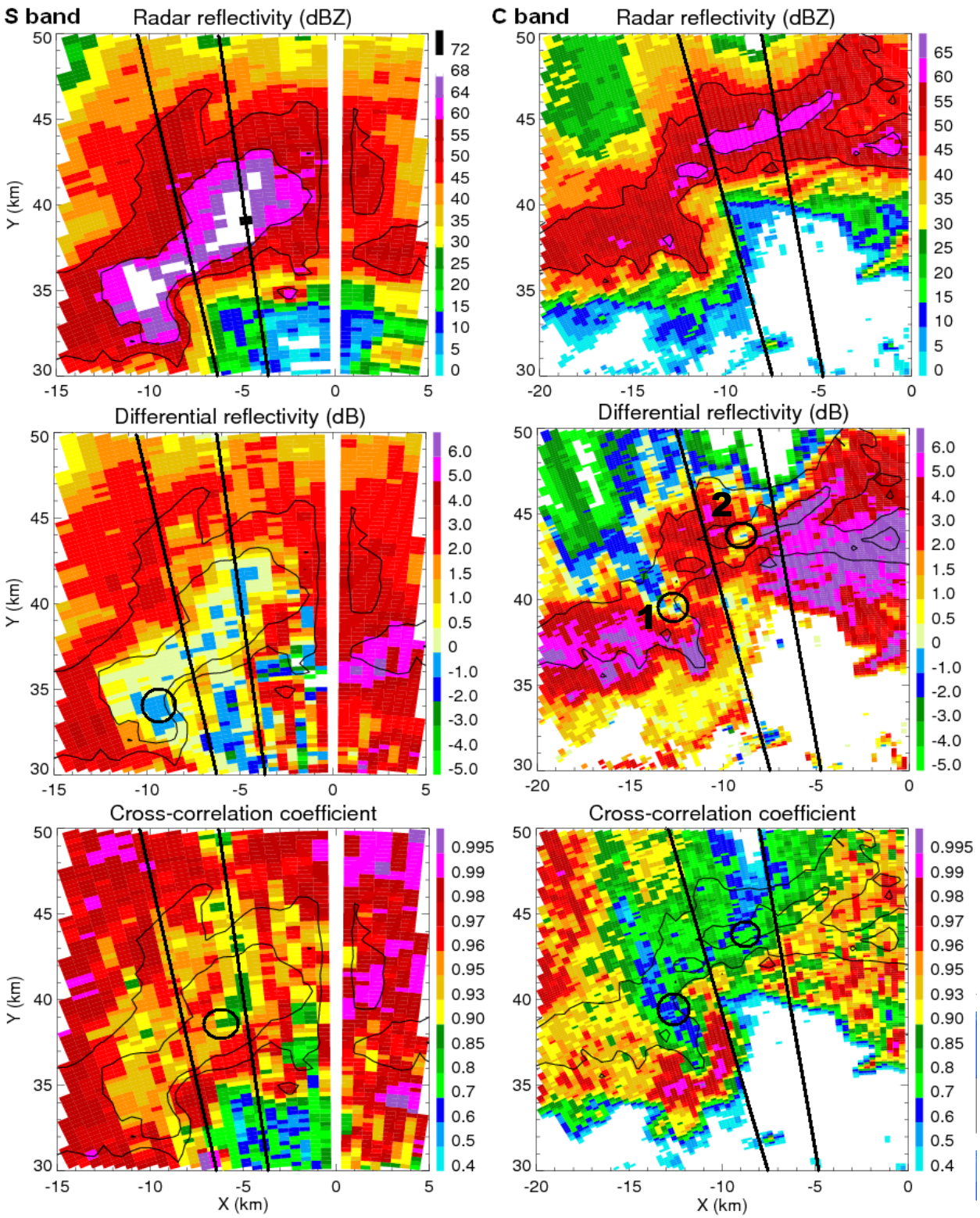

Fig. 2: KOUN (S band) and OU-PRIME (C band) 2059 UTC 0.5˚ and 2100 UTC 0.25˚ PPIs, respectively, of Z_H (top) from 16 May 2010 and corresponding PPIs of Z_{DR} (middle) and ρ_{hv} (bottom). C band highlighted regions 1 and 2 are labeled in Z_{DR} plot. Black lines display the radials from which the polarimetric values are displayed in Fig. 4.

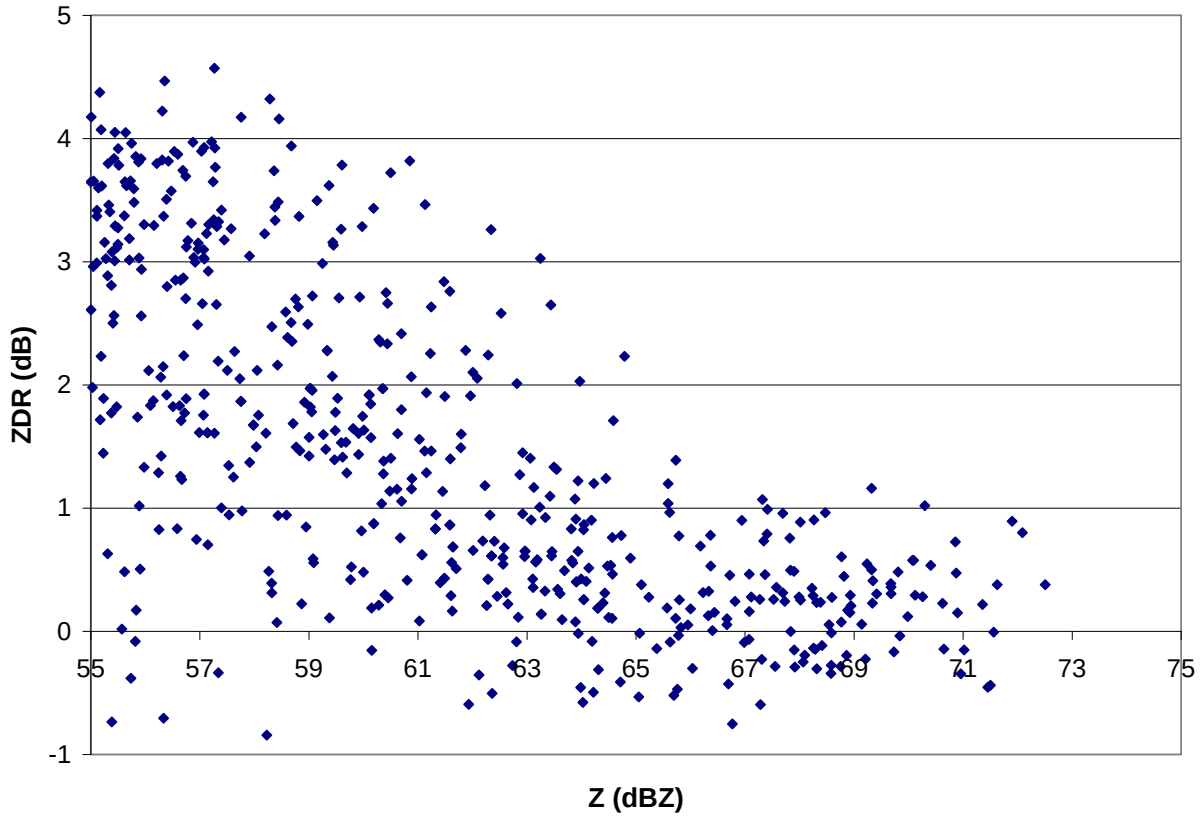

Fig. 3: Z_H-Z_{DR} scatterplot from the KOUN 0.5˚ elevation scan of the supercell at 2059 UTC for gates with Z_H > 55 dBZ. The approximate beamheight is 0.3 km above ground.

radials pass through the highlighted regions in Fig. 2, they still carry significance for their location. The first pair of azimuths (KOUN - 348˚, OU-PRIME - 346˚) passes through the inflow region where an abundance of large raindrops is not expected. Conversely, the second pair (KOUN - 353˚, OU-PRIME - 351˚) passes through the Z_{DR} arc, which is notorious for the presence of large drops. Indeed, their presence is quite apparent by the high Z_{DR} along the forward-flank Z_H gradient. Therefore, as the two pairs pass through regions of the supercell with distinct hydrometeor type and size distributions, unique insight into the microphysical properties is gained.

Fig. 4 displays radial profiles of the polarimetric variables shown in Fig. 2. The comparison on the left side aims to highlight Z_{DR} and ρ_{hv} values at both wavelengths for a large hail signature (around 37 km range). At this range, we note high Z_H around 65 dBZ and 60 dBZ for S and C bands, respectively, as well as low Z_{DR} (around 1 dB at C band and 0 dB at S band). Additionally, there is a depression in ρ_{hv} to 0.95 at S band and below 0.7 at C band. Based on the low, but not negative, values of Z_{DR} and the depressed ρ_{hv} values, it seems clear that both radars are observing severe, but not giant, hailstones around 3-5 cm diameter. This conclusion agrees with the location of these radials, as they cut between the two highlighted giant hail regions in Fig. 2.

Additionally, the largest difference in Z_H between S and C bands is found near the peak in reflectivity (around 37 km range), representing the "hail signal" previously discussed. However, at its greatest magnitude the difference is only 5 dBZ, likely not representative of giant hailstones. Moreover, only 1-2 km behind this maximum, S- and C-band Z_H values tend to converge, indicating a switch to primarily small, rapidly melting hail and large drops.

Further supporting this conclusion, C band Z_{DR} "spikes" to approximately 3 dB on both sides of the hail signal, which indicates smaller, melting hailstones (< 3 cm) whose near-0 dB contribution is overwhelmed by higher Z_{DR} values resulting from large liquid drops.

The most apparent feature of the right side (farther into the forward flank) is the extreme differential attenuation at C band. Between 38 and 42 km range, C-band Z_{DR} drops below -10 dB,

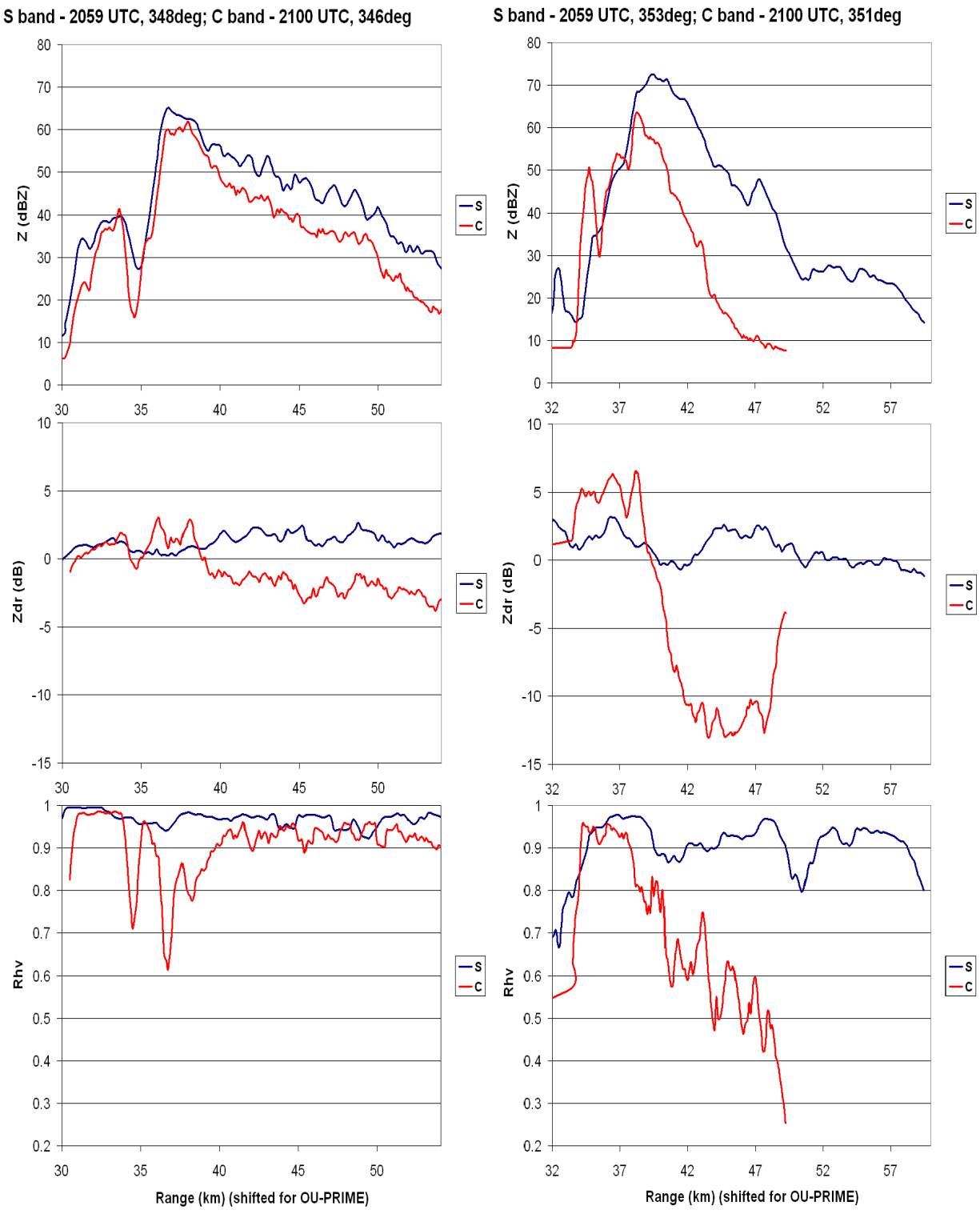

Fig. 4: Radial values of Z_H (top), Z_{DR} (middle), and ρ_{hv} (bottom) from KOUN at 2059 UTC (blue curves) at 348˚ (left) and 353˚ (right) and from OU-PRIME at 2100 UTC (red curves) at 346˚ (left) and 351˚ (right). Values are taken from the lowest elevation angle for each radar (0.5˚ for KOUN; 0.25˚ for OU-PRIME). C band values are shifted to the left by 6 km to account for the distance between the two radar sites and facilitate comparison.

due to much greater attenuation of the horizontally-polarized signal than the vertically-polarized signal. Total attenuation of the signal is also quite apparent, as Z_H peaks at 65 dBZ and then rapidly decreases with range, while S band Z_H continues rising to 72 dBZ around 39.5 km range.

Based upon S band data in this area, which indicate very large hailstones, in conjunction with very high C band Z_{DR} (> 6 dB) directly in front of this area relative to the radar site, it seems quite likely that we are observing anomalously high C-band attenuation first from abundant large drops in the Z_{DR} arc and then from a mixture of numerous hailstones, including sizes ranging from very large (near 5 cm or slightly greater) to smaller, more rapidly melting hailstones.

When considering the location of this region within the far forward flank of the hail core, it seems unlikely that extremely large hailstones (> 7 cm) were falling in this region. However, as will be seen in the next section, the supercell's updraft was promoting significant wet hail growth well into the forward flank of the storm. Therefore, the polarimetric variables are most likely indicating an extreme number of damaging hailstones, which would agree with reports of "hail drifts" exceeding 1 m in height. Additionally, when C band Z_H peaks, the Z_H difference between the two profiles is 6-7 dBZ, which is slightly greater than with the previous radial pair. Therefore, this hail signal further supports the belief that hail sizes are slightly larger in this region than in the previous one. Although S band Z_H increases to 72.5 dBZ at 39.5 km range, attenuation becomes too great at C band to continue comparing Z_H values accurately in this manner.

These analyses of attenuation parameters at C band provide new insight into the microphysical properties of precipitation. And when S band data are also available, as they were with 16 May 2010, this insight can then be applied to these data as well, improving our understanding of the polarimetric variables and providing a route for improved classification algorithms.

2.3 Hail Growth Region

In addition to the numerous reports of hail damage, the supercell's ability to produce an extreme number of hailstones across a wide swath is evidenced by a brief S band analysis of the wet growth region in the minutes prior to 2100 UTC.

Previous research has found that depressions in ρ_{hv} above the freezing level often indicate the presence of both liquid water and ice (Ryzhkov et

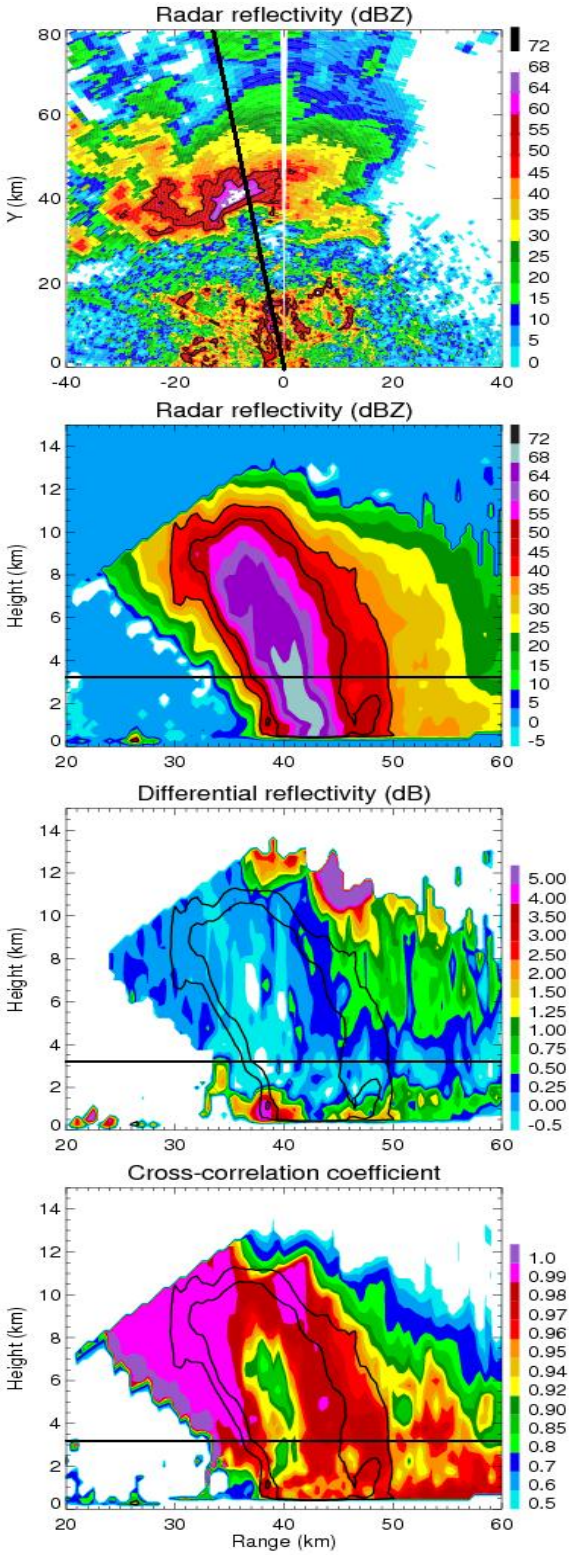

Fig. 5: KOUN 0.5˚ PPI from 2055 UTC and corresponding RHIs (351˚ - indicated on PPI) of Z_H, Z_{DR}, and ρ_{hv} below the PPI. Approximate environmental freezing level of 3.2 km AGL is indicated by horizontal lines on RHIs.

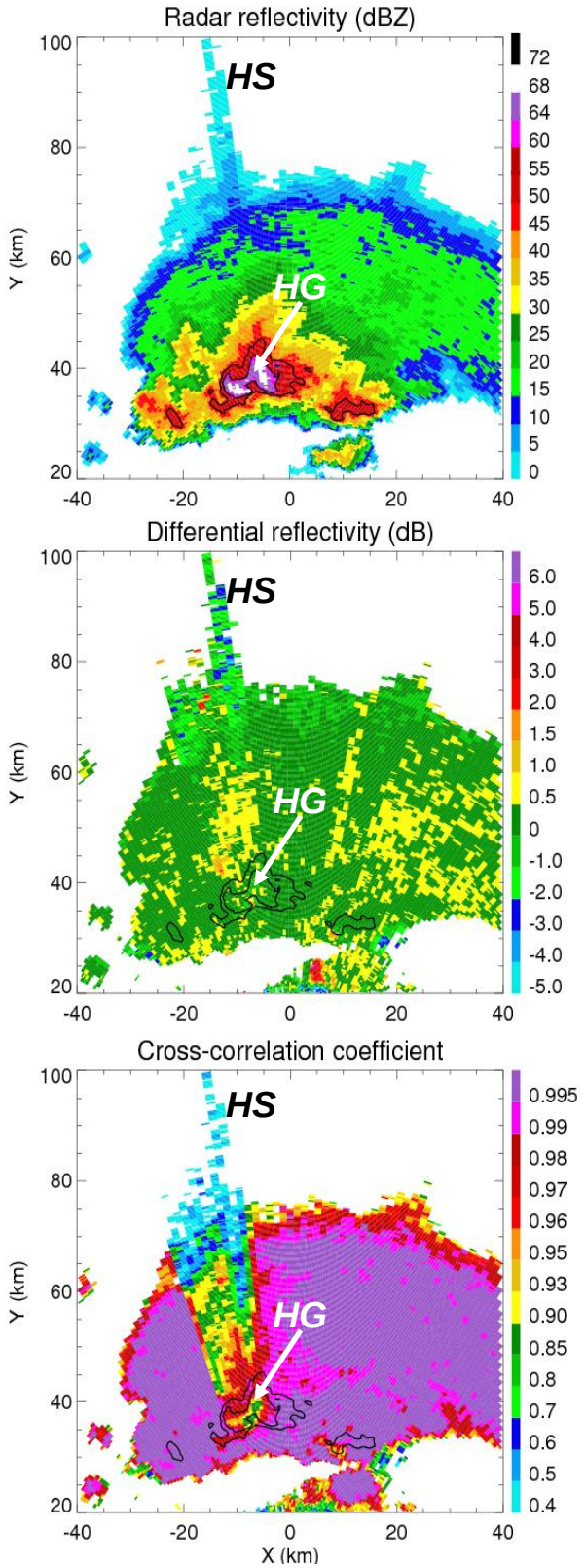

Fig. 6: KOUN 2055 UTC 8.0˚ PPI of Z_H (top), Z_{DR} (middle), and ρ_{hv} (bottom). The hail growth (HG) and hail spike (HS) signatures are highlighted.

al. 2005; Kumjian and Ryzhkov 2008). This mixture allows for hailstones to rapidly accumulate mass in a wet growth regime, as the hailstones can capture both supercooled liquid water and ice particles. Additionally, a reduction in ρ_{hv} is associated with hydrometeors reaching resonant-scattering sizes. Therefore, low values (generally < 0.9 at S band) above the freezing level also tend to indicate hailstones reaching sizes of 4-5 cm and greater.

Moreover, Z_{DR} values falling near or below 0 dB likely indicate the presence of "giant" hailstones (≥ 5 cm), regardless of the stones being wet or dry (Ryzhkov et al. 2010).

With these polarimetric characteristics in mind, viewing a PPI and RHI from 2055 UTC quickly illustrates the incredible hail production of this storm (Figs. 5-6). Typically in stronger hail-bearing cells, a combination of such Z_{DR} and ρ_{hv} values is found near the top of the main updraft and not extending significantly into the forward flank of the cell (Ryzhkov et al. 2005; Kumjian and Ryzhkov 2008). However, Fig. 5 displays the sheer magnitude of the significant hail growth region. RHIs of previous cases involving polarimetric analyses of significant hailstorms have indicated a tendency for the mixed phase growth region, where hailstones gain mass most rapidly, to diminish in size and intensity as the azimuth is shifted farther into the forward flank and away from the main updraft (Picca and Ryzhkov 2010). However, even at 351˚ KOUN data indicate efficient growth of numerous damaging hailstones, with negative Z_{DR} and ρ_{hv} < 0.9 extending over a significant volume. During the next several minutes, the descent of this hail core would result in excessive damage to buildings, automobiles, and vegetation across northwest portions of the metropolitan area.

Fig. 6 further highlights the very large region of growing hailstones, which are capable of significant damage, that extends well into forward flank. These hailstones eventually reached the ground over a wide swath of northwest Oklahoma City, including the Penn Square Mall area, causing an extreme amount of damage. Moreover, ρ_{hv} < 0.93 extends to the western edge of the 60 dBZ contour. Even in this region, hailstones reaching severe criteria (> 2.5 cm) are almost certainly being produced.

2.4 Three-Body Scatter Spike

Three-body scatter spikes (TBSS), or "hail spikes," have frequently been observed and discussed in the literature (e.g., Zrnić 1987). Their

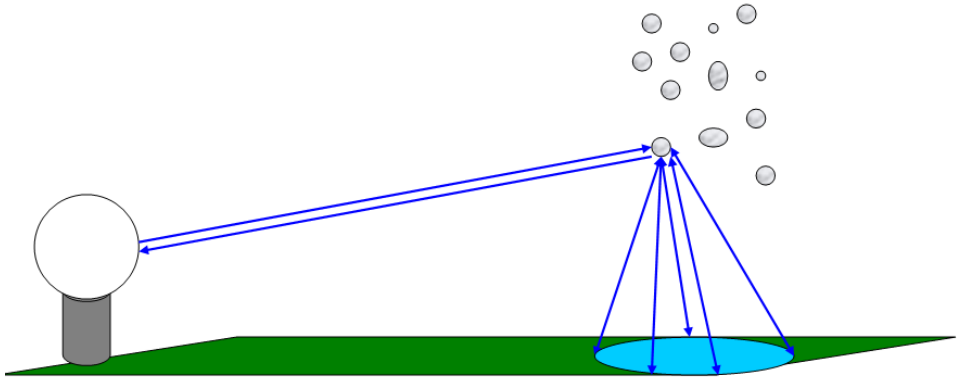

Fig. 7: Schematic illustrating the path of the electromagnetic radiation that contributes to the TBSS pattern: from the radar to the hailstones, the hailstones to the ground, the ground back to the hailstones, and finally the hailstones back to the radar. Rather than the classic schematic of the downscattered signal being only in the vertical, this image represents a more realistic case of returns coming from a conical region underneath the hailstones (Kumjian et al. 2010b).

appearance on conventional single-polarized radar typically consists of a radial extension of low Z_H behind an intense hail core, relative to the radar site.

With dual-polarized radar, this Z_H extension usually coincides with high Z_{DR} and very low ρ_{hv}, due to the process by which the radar signal is scattered to the ground and then back to the hailstone and eventually the radar itself. Normally, this radial extension is approximately 10-30 km (Lemon 1998), owing to the increased distance the signal must travel. The farther the TBSS extends radially, the greater the area encompassed by a conical region of returns beneath the hailstone (Fig. 7; Kumjian et al. 2010).

Truly displaying the incredible nature of this case, Fig. 6 exhibits a TBSS (originating around 40 km in range at an approximate height of 5.3 km AGL) that extends nearly 60 km from the hail core. To achieve this distance, backscattered returns must be occurring over a very large conical region. In turn, it becomes clear that the elevated hail core at this time had to contain such a great number of very large hailstones that the downscattered signals on the outside of this conical region were still strong enough to undergo three-body scattering and be detected by radar. The extreme length of this TBSS also explains the negative Z_{DR} beyond 70 km range. To achieve these ranges, scattering theory dictates that a majority of the returns must be from the vertically-polarized signal (see Kumjian et al. 2010 report for further explanation). At closer ranges, Z_{DR} is higher, although not as high as is typically seen with TBSS signatures. Due to the presence of frozen hydrometeors in this region (with intrinsic Z_{DR} generally near 0 dB), the very high Z_{DR} of the TBSS is masked.

3. GROUND TRUTH HAIL REPORTS

Perhaps the most important, yet also unfortunate, aspect of this event is its path over a highly populated, well-developed metropolitan area. Although damage costs are estimated to be in the hundreds of millions of dollars, the number of people in the storm's path also allowed for numerous in-situ hail reports. While some uncertainty lies in the exact time and hail size within these reports, the high quality of radar data and specificity of the location of many reports (due to being within an urbanized road network) were sufficient to match with confidence individual reported hail sizes with specific range gates. Therefore, this study is able to compare KOUN polarimetric data from different regions of the supercell with various hail sizes, ranging from 2.5 cm upwards of 8 cm.

Three scatterplots (Z_H-Z_{DR}, Z_H-ρ_{hv}, and Z_{DR}-ρ_{hv}) comparing data from the 0.5° scan are produced to illustrate the importance of utilizing multiple polarimetric parameters to estimate hail location and size with the greatest degree of accuracy possible (Figs. 8-10). To allow for possible slight inaccuracies in the time or location of the reports, all range gates (with $Z_H \geq 55$ dBZ) within 1° azimuthally and 1 km radially of the coordinates of the report were plotted for that hail size. In total, 13 reports were used, with seven different size categories (2.5 cm, 4.4 cm, 5 cm, >5 cm, 6.4 cm, > 6.4 cm, and 8 cm).

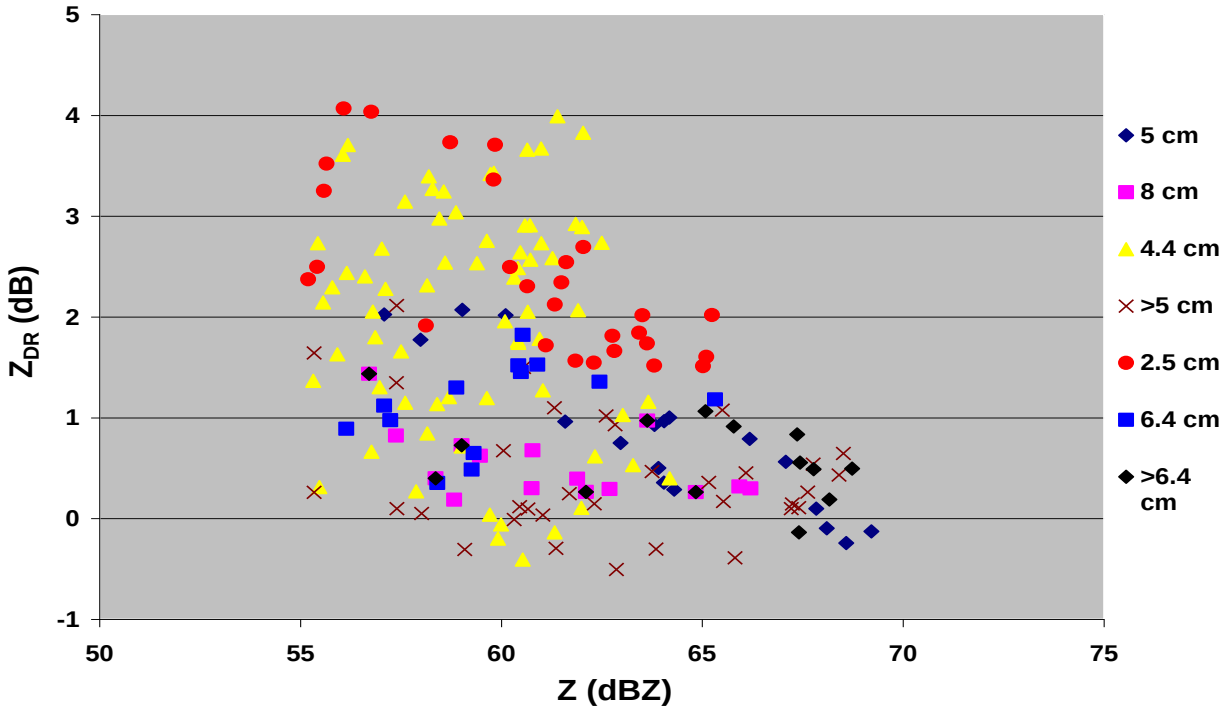

Fig. 8: Scatterplot of Z_H vs Z_{DR} values from 13 hail reports between 2058 and 2129 UTC across the Oklahoma City metro area.

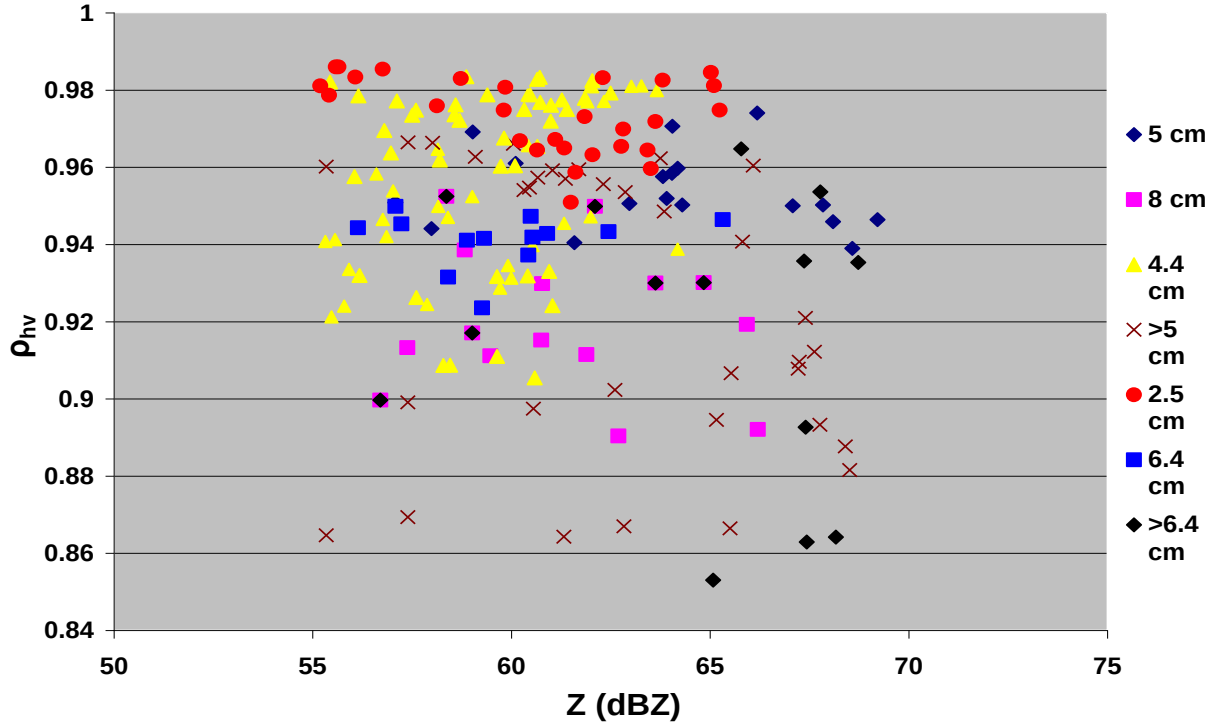

Fig. 9: Same as for Fig. 8, except a scatterplot of Z_H vs ρ_{hv}.

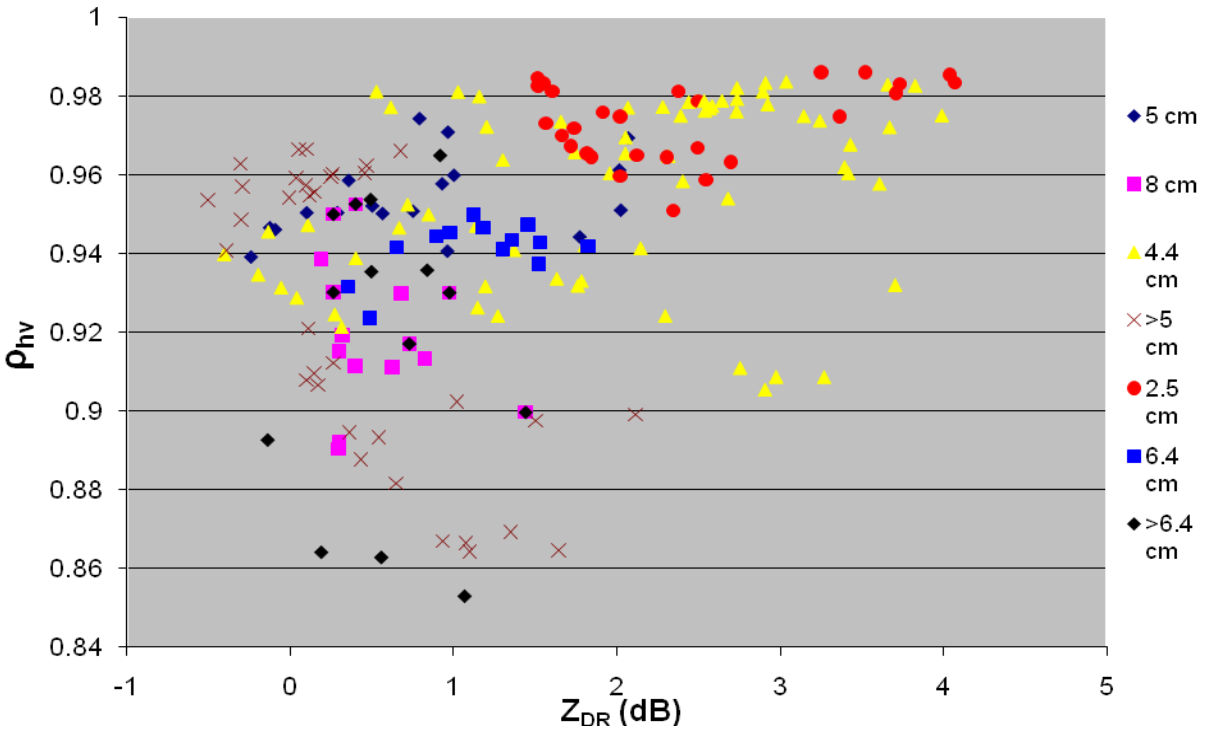

Fig. 10: Same as for Fig. 8, except a scatterplot of Z_{DR} vs ρ_{hv}.

For both the Z_H-Z_{DR} and Z_H-ρ_{hv} plots, there is a clear trend of larger hail sizes towards increasing Z_H and decreasing Z_{DR} or ρ_{hv}. Fig. 8 shows that when Z_H > 65 dBZ and Z_{DR} < 1 dB, all data points are giant hail reports, illustrating the general success of Z_{DR} at identifying regions of hail. However, where Z_H is between 55 dBZ and 65 dBZ and Z_{DR} between 0 dB and 2 dB, there is a wide array of hail size data points, indicating the need for better size discrimination if improved hail-sizing algorithms are to be achieved.

The Z_H-ρ_{hv} scatterplot has similar characteristics (Fig. 9). When Z_H > 65 dBZ and ρ_{hv} < 0.95, all data points are giant hail reports, exhibiting that ρ_{hv} also has success at identifying regions of hail. Yet again, however, where Z_H is between 55 dBZ and 65 dBZ and ρ_{hv} between 0.9 and 0.96, there is a greater distribution of hail sizes. Therefore, while also an improvement over the use of just Z_H, ρ_{hv} (in combination with Z_H) does not provide the discrimination capabilities to offer a substantial upgrade over current algorithms.

Finally, the Z_{DR}-ρ_{hv} scatterplot points towards the utilization of both Z_{DR} and ρ_{hv}, along with Z_H, to most accurately estimate hail size (Fig. 10). A clear trend of larger hail sizes towards lower Z_{DR} and ρ_{hv} values exists. This trend is especially noticeable when considering the 2.5 cm data points against the larger sizes. None of these marginally severe sizes display Z_{DR} and ρ_{hv} values less than 1 dB and 0.95, respectively. Conversely, a large majority of the "giant" reports fall within values less than 1 dB and 0.96. The discrimination abilities of Z_{DR}, in conjunction with Z_H, for hail detection and sizing have been well detailed in the literature (Bringi and Chandrasekar 2001). And limited validation studies have shown good skill of this method at S band (Heinselman and Ryzhkov 2006; Depue et al. 2007). However, this scatterplot certainly supports the idea that ρ_{hv} can be combined with Z_{DR} to further improve these size estimates. Future algorithms should take advantage of the ability of ρ_{hv} to highlight range gates where resonant scatterers (which are often very large hailstones in cases such as this one) are present.

Even with a combination of Z_{DR} and ρ_{hv}, however, there exists some ambiguity around an "overlap" hail size, specifically the 4.4 cm reports. With this size, we note a large range of Z_{DR} and ρ_{hv} values, with a significant number falling in the Z_{DR} > 2 dB range. The importance of these values is that they indicate that even in regions containing severe hailstones upwards of golfball sizes, other melting hailstones and large liquid drops can still mask the lower Z_{DR} of the largest hailstones within a sampling volume. Therefore, even at S band, it

appears it is not entirely necessary for low Z_{DR} to be present when large hailstones are falling. However, as hailstones approach giant sizes of 5 cm and greater, it is unlikely that Z_{DR} would remain above 2 dB.

4. CONCLUSION

The damage imposed by the 16 May 2010 Oklahoma City hailstorm was extremely costly and will continue to impose a financial burden upon many residents and businesses for the coming months and perhaps longer, as numerous repairs to vehicles and buildings are ongoing. For these reasons, the path of the storm was quite unfortunate. At the same time, a hailstorm of this magnitude passing over a metropolitan area and being sampled at relatively close ranges by two high-quality, nearly collocated polarimetric radars of different wavelengths has simply never occurred. The dataset acquired is truly "one of a kind," especially due to the high number of ground-truth hail reports.

The presence of both S- and C-band radars enables direct comparison of data of two wavelengths which provides an improved image of the types and sizes of hydrometeors falling in the precipitation core. For example, only in regions of the largest hailstones did C band Z_{DR} fall below 1 dB. Elsewhere, the magnified effect (at C band) of resonant scattering boosted Z_{DR}, while Z_{DR} remained relatively low at S band. Therefore, it becomes apparent that our knowledge of the polarimetric values resulting from various hydrometeors at C band can be used to analyze more accurately the observed values at S band.

With such a unique dataset, this case also bolsters previous findings that $Z_{DR} < 1$ dB and $\rho_{hv} < 0.95$, within a region of high Z_H, indicates the presence of very large hail (> 4 cm). Conversely, $Z_{DR} > 1$ dB and $\rho_h > 0.95$ generally indicates smaller sizes, although the presence of melting hailstones and liquid water can produce these values even when hail diameters upwards of 4 cm are present. Due to this ambiguity, more cases must be analyzed, along with continued modeling of the scattering properties of hailstones and the resultant polarimetric values.

5. ACKNOWLEDGEMENTS

We would like to thank the NSSL/CIMMS employees who ensure data collection by KOUN at research-grade quality. OU-PRIME is maintained and operated by the Atmospheric Radar Research Center (ARRC) at the University of Oklahoma. Additionally, we thank Dr. Valery Melnikov for his invaluable work in processing and analyzing the KOUN data. Funding for this study comes from NOAA/Univ. of Oklahoma Cooperative Agreement NA17RJ1227 under the U.S. Dept. of Commerce.

6. REFERENCES

Atlas, D., and F.H. Ludlam, 1961: Multi-wavelength radar reflectivity of hailstorms. *Quart. J. Roy. Meteor. Soc.*, **87**, 523-534.

Aydin, K., T. Seliga, and V. Balaji, 1986: Remote sensing of hail with a dual linear polarization radar. *J. Appl. Meteor.*, **25**, 1475-1484.

Balakrishnan, N., and D.S. Zrnić, 1990: Use of polarization to characterizer precipitation and discriminate large hail. *J. Atmos. Sci.*, **47**, 1525-1540.

Borowska, L., A.V. Ryzhkov, D.S. Zrnić, C. Simmer, R.D. Palmer, 2010: Attenuation and differential attenuation of the 5-cm wavelength radiation in melting hail. *J. Appl. Meteor. Climatol.*,**accepted**.

Bringi, V.N. and V. Chandresekar, 2001: Polarimetric Doppler weather radar. *Principles and applications.* Cambridge University Press, 636 pp.

Depue, T., P. Kennedy, and S. Rutledge, 2007: Performance of the hail differential reflectivity (H_{DR}) polarimetric hail indicator. *J. Appl. Meteor. Clim.*, **46**, 1290-1301.

Eccles, P.J., and D. Atlas, 1973: A dual-wavelength radar hail detector. *J. Appl. Meteor.*, **12**, 847-854.

Heinselman, P. and A.V. Ryzhkov, 2006: Validation of polarimetric hail detection. *Wea. Forecasting*, **21**, 839-850.

Lemon, L.R., 1998: The radar "three-body scatter spike": An operational large-hail signature. *Wea. Forecasting*, **13**, 327-340.

Kumjian, M.R., and A.V. Ryzhkov, 2008: Polarimetric signatures in supercell thunderstorms. *J. Appl. Meteor. Climatol.*, **47**, 1940-1961.

Kumjian, M.R., and A.V. Ryzhkov, 2008b: Storm-relative helicity revealed from polarimetric radar observations. *J. Atmos. Sci.*, **66**, 667-685.

Kumjian, M.R., J.C. Picca, S.M. Ganson, A.V. Ryzhkov, J. Krause, D.S. Zrnić, and A. Khain, 2010: Polarimetric characteristics of large hail. Extended Abstracts, *25th Conference on Severe Local Storms*, Denver, CO, Amer. Meteor. Soc., 11.2.

Kumjian, M.R., J.C. Picca, S.M. Ganson, A.V. Ryzhkov, and D.S. Zrnić, 2010b: Three body scattering signatures in polarimetric radar data. NOAA/NSSL report, 12 pp. Available online at: http://publications.nssl.noaa.gov/wsr88d_reports/FINAL_TBSS.doc

Picca, J.C., and A.V. Ryzhkov, 2010: Polarimetric signatures of melting hail at S and C bands: Detection and short-term forecast. Extended Abstracts, *26th Conference on Interactive Information and Processing Systems (IIPS)*, Atlanta, GA, Amer. Meteor. Soc., 10B.4.

Ryzhkov, A.V., D.S. Zrnić, P. Zhang, D. Hudak, J.L. Alford, M. Knight, and J.W. Conway, 2007: Validation of polarimetric methods for attenuation correction at C band. Extended Abstracts, *33rd Conf. Radar Meteorology*, Cairns, Australia, Amer. Meteor. Soc., CD-ROM P11B.12.

Ryzhkov, A.V., T.J. Schuur, D.W. Burgess, P.L. Heinselman, S.E. Giangrande, and D.S. Zrnić, 2005: The joint polarization experiment: Polarimetric rainfall measurements and hydrometeors classification. *Bull. Amer. Meteor. Soc.*, **86**, 809-824.

Ryzhkov, A.V., D.S. Zrnić, J. Krause, M.R. Kumjian, and S. Ganson, 2010: Discrimination between large and small hail, final report. NOAA/NSSL report, 18 pp. Available online at: http://publications.nssl.noaa.gov/wsr88d_reports/FINAL_HailSize.doc

Zrnić, D.S., 1987: Three-body scattering produces precipitation signatures of special diagnostic value. *Radio Sci.*, **22**, 76-86.